Influence of atomic termination on the $LaAlO_3/SrTiO_3$ interfacial polar rearrangement

A. Rubano,[1,2] T. Günter,[1] T. Fink,[1] D. Paparo,[2,*] L. Marrucci,[2] C. Cancellieri,[3,4] S. Gariglio,[3] J.-M. Triscone,[3] and M. Fiebig[1,5]

[1]*Helmholtz-Institut für Strahlen- und Kernphysik, Universität Bonn, Nussallee 14–16, 53115 Bonn, Germany*

[2]*CNR-SPIN and Dipartimento di Fisica, Università di Napoli "Federico II", Complesso Universitario di Monte Sant'Angelo, Via Cintia, 80126 Napoli, Italy*

[3]*Département de Physique de la Matière Condensée, University of Geneva, 24 Quai Ernest-Ansermet, 1211 Genève 4, Switzerland*

[4]*Swiss Light Source, Paul Scherrer Institut, CH-5232 Villigen, Switzerland*

[5]*Department of Materials, ETH Zurich, Wolfgang-Pauli-Strasse 10, 8093 Zurich, Switzerland*

(Received 18 February 2013; published 2 July 2013)

We report the results of second-harmonic optical spectroscopy of $LaAlO_3$ films grown on $SrTiO_3$ (001) substrates having either TiO_2 or SrO atomic terminations. The atomic termination is found to have a large effect on the observed spectra, with a strong dependence on the ω-2ω light polarizations. These results are analyzed through a model based on symmetry-controlled selection rules and atomic orbital overlaps. The analysis shows that, as suspected from transport measurements, the SrO termination prevents the formation of a mobile interfacial electron gas. Yet, by explicitly probing and identifying the electronic states at the O^{2-}–Ti^{3+} band gap we now obtain unique and direct evidence that this is caused by the absence of any detectable charge injection in the interfacial region rather than by carrier localization.

DOI: 10.1103/PhysRevB.88.035405 PACS number(s): 73.20.−r, 42.65.Ky, 73.40.−c, 77.22.Ej

I. INTRODUCTION

The discovery of a two-dimensional electron gas (2DEG) formed, under specific conditions, at the interface between the two band insulators $LaAlO_3$ (LAO) and $SrTiO_3$ (STO),[1] has triggered an intense research effort. It is unveiling a surprising array of unexpected phenomena, ranging from tunable conductivity to 2D superconductivity.[2] The origin of the charge carriers has been a much debated question, since different intrinsic and extrinsic doping mechanisms, such as cation intermixing and vacancy defects, can be at play in this oxide heterostructure.[3–11] Many recent results point to the so-called *polar catastrophe scenario* as the mechanism driving the formation of the conducting state.[3,11–15] According to this picture, the polar discontinuity that occurs at the interface between the charge-neutral planes of SrO and TiO_2 and the charged LaO ($+e$, where e is the electron charge) and AlO_2 ($-e$) sheets brings about an electrostatic breakdown once the $LaAlO_3$ layer has reached a critical thickness. This model is well verified in many aspects, but, being a very crude model, several discrepancies are found that make this controversy still alive.

The 2DEG is actually observed only in heterostructures formed with TiO_2-terminated STO (n-type, TiO_2/LaO interfaces). When the STO substrate is terminated with a SrO plane, resulting in a SrO/AlO_2 interface, a p-type conductive interface is expected based on the polar catastrophe hypothesis, but, experimentally, the samples are found to be insulating.[1,3] Various models referring to this observation are controversially discussed. The insulating state of the interface might result from a lack of electronic reconstruction, with other mechanisms hence balancing the polar discontinuity at the interface. Alternatively, the SrO-terminated heterostructure, compared with the TiO_2-terminated one, may be more prone to charge localization, caused, for instance, by the difference in defects or disorder expected at the differently terminated interface. In this case an electronic reconstruction at the interface could still occur, but because of such an increased localization it would not be visible to transport measurements.

As additional complication, it has been recently argued that charge injection in TiO_2-terminated LAO/STO interfaces is not the only reconstruction mechanism occurring to reduce the potential buildup in thin LAO overlayers, but that the latter is also partially compensated by ionic displacements occurring in both LAO and STO.[16] Hence it would be desirable to verify the occurrence of the ionic displacement at the conducting and the insulating interfaces.

To achieve a comprehensive understanding of the microscopic mechanisms leading to the 2DEG, all the aforementioned issues must be further examined. Most studies investigating the formation of the 2DEG rely on transport measurements, which detect mobile carriers only. Hence, these techniques do not provide useful information when insulating systems are considered. Only a spectroscopic method can reveal the arrangement of the interfacial electronic structure and the orbitals involved, providing access to the microscopic mechanisms triggering the 2DEG formation.

In this work we make use of optical second harmonic generation (SHG) spectroscopy for shedding light on the role of the atomic termination in the physics of LAO/STO interface. We find that electron charge injection does not occur at the SrO-terminated interface, which is also the reason for the persistence of the insulating state. We establish the band structure of the Ti and O states at the band gap and show how the corresponding electronic orbitals are affected by the interface with respect to the termination.

II. PROBING $LaAlO_3/SrTiO_3$ INTERFACES BY SHG

SHG denotes the generation of an optical wave with frequency 2ω by an incident wave of frequency ω. This process is determined by the constitutive relation $P_i(2\omega) = \varepsilon_0 \chi_{ijk} E_j(\omega) E_k(\omega)$, where $\mathbf{P}(2\omega)$ is the induced second-order optical polarization, $\mathbf{E}(\omega)$ the electric field of the incident

wave, and $\hat{\chi}$ the SHG susceptibility tensor. The SHG intensity I_{SHG}, as measured experimentally, is proportional to the square of the reflected SHG electric field: $I_{\mathrm{SHG}} \propto |\mathbf{P}(2\omega)|^2$.

Recently the coupling of optical SHG to the interfacial reorganization of LAO/STO interfaces was demonstrated.[18–21] The SHG signal requires a breaking of the inversion symmetry and thus is an ideal tool for investigating the polar asymmetry developed at an interface. Compared to standard optical techniques, an advantage of SHG is that its probing depth is not *a priori* fixed, but depends on the space extension of the polar asymmetry at the specific interface. Therefore it only senses the interfacial property of interest here with background-free capability. Previous experiments already showed a decoupling between the change of conductance and the actual orbital reconstruction preceding it. This distinction was only possible by directly probing the electronic states optically instead of resorting to transport experiments. Thus, we will adhere to the same methodology in the present system. We will furthermore use SHG selection rules in order to identify and distinguish the electronic states determining the properties at the LAO/STO interface.

III. EXPERIMENT

LAO films of five unit cells were prepared by pulsed laser deposition (PLD) on (001)-oriented STO substrates with uniform TiO_2 or SrO terminations. SrO-terminated substrates were obtained by depositing a SrO layer on a TiO_2-terminated STO crystal before growing *in situ* the LAO film. The thickness of the layers was monitored during the deposition using reflection high-energy electron diffraction (RHEED) oscillations as shown in Fig. 1. This allows a precise control of the layer-by-layer growth. The samples were grown at 800 °C in 1×10^{-4} mbar of oxygen atmosphere; annealing in 0.2 bar of oxygen at 550 °C for one hour precedes the cool-down to room temperature at the same pressure.[14] The films grown on TiO_2-terminated STO are conductive, with a sheet conductance of about $\sigma_S = 0.05$ mS at 300 K, while the samples grown on SrO-terminated STO display a sheet conductance below the detection limit of 10^{-9} S.

For the optical investigation, frequency-tunable laser pulses of 130 fs were generated at 1 kHz by an optical parametric

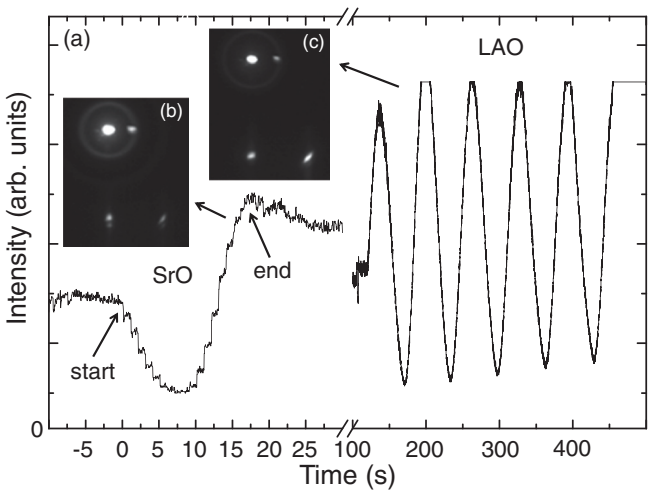

FIG. 1. RHEED oscillations for the growth of five monolayers of $LaAlO_3$ onto SrO-terminated substrate. To obtain the latter a monolayer of SrO is grown on TiO_2-terminated $SrTiO_3$ substrate prior to the $LaAlO_3$ deposition. Panels (b) and (c) show the final RHEED patterns after SrO and $LaAlO_3$ deposition, respectively. The RHEED intensity is measured at the specular spot for the SrO layer, while it is measured on the (0 1) diffraction spot for the $LaAlO_3$ film, thus explaining the phase shift. RHEED oscillations for $LaAlO_3$ layer growth on TiO_2-terminated surfaces can be seen in Ref. 17.

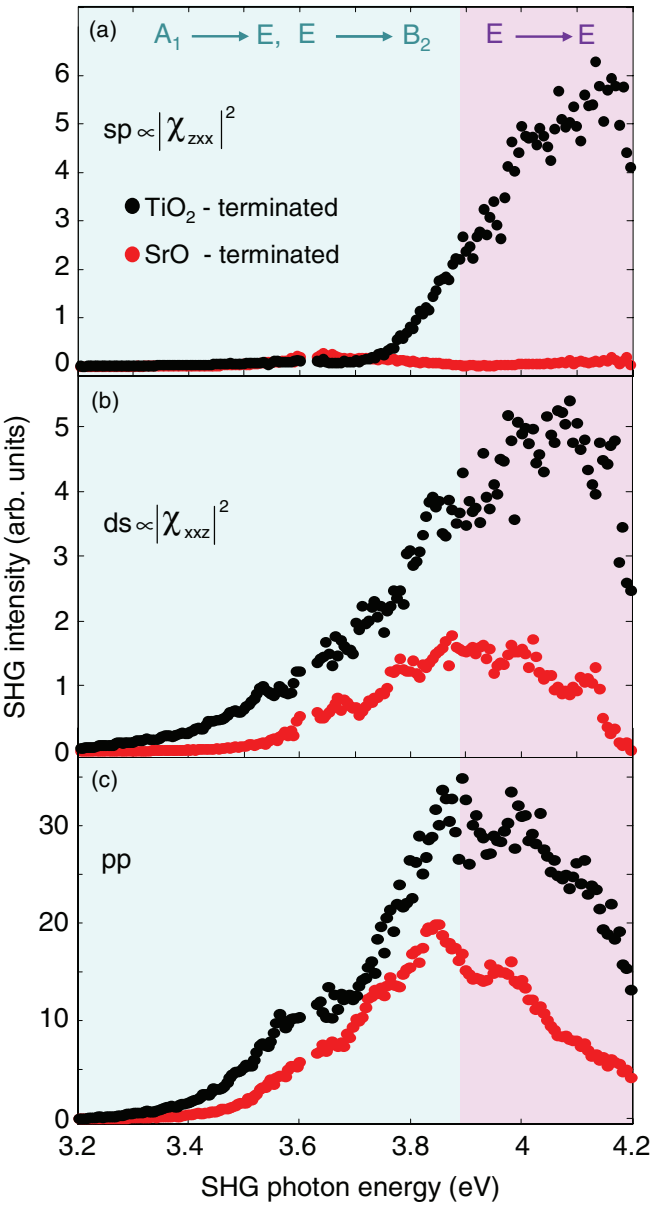

FIG. 2. (Color online) Comparison of SHG spectra from LAO/STO heterostructures with five unit cells of LAO and different interfacial atomic terminations. The labels *sp* (a), *ds* (b), and *pp* (c) refer to different ω-2ω polarization combinations (see text). The spectra for the SrO-terminated substrate (red symbols) are multiplied by a factor 4 for better visibility. The colored areas divide the plot into two energy ranges corresponding to the identified electronic transitions: the blue area is dominated by $A_1 \rightarrow E$, $E \rightarrow B_2$ transitions, while the purple area is guided by $E \rightarrow E$ transitions, as shown in Fig. 3.

amplifier pumped by a Ti:sapphire amplifier system. Both the input fundamental and the output SHG beam are linearly polarized. In the following, the labels p, s, and d are used to denote linear polarizations parallel, perpendicular, or at 45° with respect to the plane of incidence of light. In accordance with the fourfold rotational symmetry of the interface, we observed only three independent nonvanishing SHG components: p-in p-out (pp), s-in p-out (sp) and d-in s-out (ds).[20]

IV. RESULTS

Figure 2 shows representative SHG spectra in the SHG photon-energy range between 3.2 and 4.2 eV obtained for the two atomic terminations at the three aforementioned polarization combinations (below 3.2 eV, all SHG spectra are featureless). We analyzed several samples for both terminations, finding reproducible results. Let us first focus on the TiO_2-terminated samples. The main peak of the pp SHG spectrum at about 3.8–4.0 eV is ascribed to the known valence-to-conduction band edge.[22] At 3.6 eV, an additional peak is present that was previously attributed to a surface subband.[20] Interestingly, this peak is completely absent in the sp spectrum, clear evidence of the action of a symmetry selection rule. Turning to the SrO-terminated interface, we first note a drastic decrease of the SHG signal in all spectra. The SHG intensity is comparable to that obtained from bare STO surface or n-type samples with one unit cell of LAO (data not shown). In addition, the sp spectrum shows a complete suppression of the peak at 3.8–4.0 eV. This result is especially striking if one notes that, not considering possible interfacial reconstructions, the SrO-terminated system is structurally identical to the TiO_2-terminated one, except for the two half-unit cells adjacent to the interface on the LAO and STO sides. Minor modifications of the spectral shape are also found for the ds and pp spectra, as shown in Figs. 2(b) and 2(c), respectively.

V. DISCUSSION

Let us now discuss these observations in the framework of a simple model based on the orbital overlaps and selection rules involved in the various optical transitions contributing to the SHG spectra. It has been already established that the SHG source resides in the STO side of the interface.[20] Therefore we focus our attention on the STO structure and symmetries, and discuss the expected changes due to the interface-induced symmetry breaking. Moreover, since the investigated range is close to the interband transition edge, we will limit our analysis to the symmetry valid at the Γ point of the Brillouin zone. The bulk STO optical gap is associated with a transition from oxygen $2p$ to titanium $3d$-t_{2g} orbitals.[22] The valence band is dominantly composed of $2p$ oxygen orbitals, which can be qualitatively described by combining the p_x, p_y, and p_z orbitals of the three oxygen atoms of each unit cell, for a total of nine independent bands. Here we use a Cartesian reference system with the $\hat{z}$ axis perpendicular to the interface, and $\hat{x}$ and $\hat{y}$ in the interfacial plane. At the Γ point of the bulk Brillouin zone, these bands may be grouped in three levels, as shown in Fig. 3, depending on the relative arrangement of the $2p$ orbitals: bonding and antibonding, both with cubic symmetry Γ_{15}, and approximately nonbonding, with symmetry Γ_{25}.[23] Each of these levels is threefold degenerate in the bulk owing to the cubic symmetry of the crystal. The minimum optical (vertical) transition energy, located at Γ, is known to be 3.75 eV.[22] The conduction band is composed of Ti($3d$) orbitals. The cubic crystal field arising from the six nearest-neighbor O atoms splits the Ti($3d$) orbitals into three lower energy t_{2g} orbitals (xy, yz, zx) and two e_g orbitals ($3z^2 - r^2$, $x^2 - y^2$).[22] The latter ones are not further considered here, as they lie more than 2 eV above the t_{2g} band[24] and hence out of the investigated energy range. At the LAO/STO interface the symmetry is lowered from the cubic 3D symmetry $m3m$ to the quadratic 2D symmetry $4mm$, which further splits the bands at the Γ point as summarized in Fig. 3. The Ti($3d$-t_{2g}) orbitals split in two levels: d_{xy}, according to the representation B_2, and the two degenerate orbitals d_{xz} and d_{yz} forming an E doublet.[25] The oxygen orbitals at the interface are split into six distinct levels, of which one A_1 singlet and one E doublet originating from the antibonding orbitals constitute the states that are highest in energy ($\geqslant$1 eV higher than the other oxygen bands[26]).

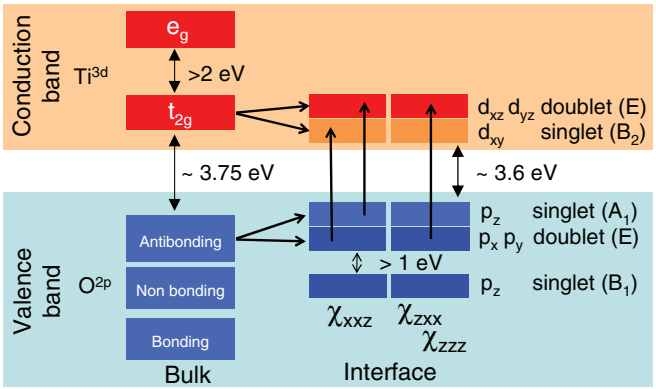

FIG. 3. (Color online) The symmetry-allowed O($2p$)-Ti($3d$) 2ω transitions for all three symmetry-allowed χ_{ijk} components within the $4mm$ symmetry group are shown. According to the selection rules the allowed transitions for χ_{zzz} (contributing to the pp signal together with the other χ elements) and χ_{zxx} (sp signal) are the same, whereas two different transitions are allowed for χ_{xxz} (ds signal).

The Ti($3d$-t_{2g}) and O($2p$) orbitals described above give rise to the resonances observed in our SHG spectra which can be ascribed to 2ω transitions from a single-electron state in the valence band to a single-electron state of the conduction band.[20] Let us now link the χ elements to specific O($2p$)-Ti($3d$) transitions. Within the $4mm$ symmetry, three independent nonvanishing tensor components for $\hat{\chi}$ are allowed, namely χ_{zzz}, $\chi_{zxx} = \chi_{zyy}$, and $\chi_{xxz} = \chi_{yyz} = \chi_{zxz} = \chi_{yzy}$. Two of them, χ_{xxz} and χ_{zxx}, can be singled out from the net SHG signal by an appropriate choice of polarization for the light at ω and 2ω. The magnitudes of χ_{xxz} and χ_{zxx} are directly proportional to the square root of the SHG intensity of the ds and sp polarization combinations, respectively. In contrast, χ_{zzz} appears only in combination with the two aforementioned susceptibilities. However, according to Fig. 3 and the following selection rules, χ_{zxx} and χ_{xxz} reveal all the relevant information so that we can focus here on these two only.

At the Γ point and for 2ω transitions between a valence-state V and a conduction-state C, a simple symmetry argument can

be used for obtaining the relevant optical selection rules. For a 2ω resonance these rules are dictated only by the parity of the first χ index, which is associated with the emission of the second harmonic photon. The index variables z and x belong to the $4mm$ group representations A_1 and E, respectively. We can use then the table of the representation direct products for the $4mm$ group, as given, for example, in Appendix B of Ref. 25, to obtain the following selection rules:

$$\chi_{zzz} \neq 0,\ \chi_{zxx} \neq 0,\ \chi_{xxz} = 0,$$
if V, C have the same symmetry,
$$\chi_{zzz} = 0,\ \chi_{zxx} = 0,\ \chi_{xxz} \neq 0,$$
if V, C have different symmetry, one being E,
$$\chi_{zzz} = 0,\ \chi_{zxx} = 0,\ \chi_{xxz} = 0,$$
if V, C have different symmetry, not E.

Let us discuss first the case of TiO_2-terminated interfaces. As already pointed out, a comparison between the sp and ds spectra in Figs. 2(a) and 2(b) reveals clear qualitative differences. In particular, the lowest energy resonance at 3.6 eV visible in the ds and pp spectra is completely absent in the sp spectra. We can hence assign it to a transition that is allowed for χ_{xxz} ($\sim ds$) and forbidden for χ_{zxx} ($\sim sp$). According to Fig. 3 possible candidates are (i) $E \rightarrow B_2$: O(p_x, p_y) $\rightarrow$ Ti-t_{2g}(d_{xy}), and (ii) $A_1 \rightarrow E$: O(p_z) $\rightarrow$ Ti-t_{2g}(d_{xz}, d_{yz}). Angle-resolved photoemission spectroscopy data on $SrTiO_3$ surfaces[27] and x-ray absorption spectroscopy[24] on LAO/STO show that the lowest conduction band is given by d_{xy} orbitals, but since the valence band is also split by an unknown value we cannot determine the relative placement of case (i) and case (ii) in the SHG spectrum. However, as we will see this distinction is not needed for the following analysis. In any case, Fig. 3 allows us to assign the higher-energy resonance in the sp SHG spectrum observed in the TiO_2-terminated interfaces around 4.0 eV unambiguously to the $E \rightarrow E$: O(p_x, p_y) $\rightarrow$ Ti-t_{2g}(d_{xz}, d_{yz}) transition.

Let us now discuss the changes observed in the SHG spectra when passing from the TiO_2 termination to the SrO one. The most striking effect is the near-full suppression of the sp signal that we ascribed to the transition $E \rightarrow E$: O(p_x, p_y) $\rightarrow$ Ti-t_{2g}(d_{xz}, d_{yz}). This cannot be explained with selection rules only, since both terminations correspond to the same interfacial symmetry. On the other hand we can propose a simple interpretation for this effect if we assume that SHG is generated mainly in the orbitals localized within a single atomic plane from the interface, as these are strongly polarized due to the structural proximity effects. With this assumption, a significant difference between the TiO_2 and SrO terminations occurs as shown in Fig. 4. In the SrO interface only the p_z oxygen orbitals have a significant overlap with the Ti($3d$) orbitals of the TiO_2 layer underneath, so that only transitions involving p_z should be pronounced in the SHG spectrum. Therefore, the $E \rightarrow E$: O(p_x, p_y) $\rightarrow$ Ti-t_{2g}(d_{xz}, d_{yz}) transition of the sp spectrum is suppressed in SrO-terminated systems. In contrast, transitions $A_1 \rightarrow E$: O(p_z) $\rightarrow$ Ti-t_{2g}(d_{xz}, d_{yz}) remain possible, and give rise to the nonvanishing ds and pp SHG spectra of the SrO-terminated sample. However, here the $E \rightarrow B_2$: O(p_x, p_y) $\rightarrow$ Ti-t_{2g}(d_{xy}) transition will be suppressed.

In contrast, in the TiO_2-terminated samples the charge injection triggering the reconstruction at the interface creates a space-charge region extending across few unit cells,[16,18,20,28] thus developing an electric field that polarizes all the orbitals involved in the SHG spectra (for example by displacing the Ti ions). Therefore, the overall SHG yield will be higher and all the O($2p$) $\rightarrow$ Ti($3d$) transitions that are allowed by symmetry will contribute to the SHG spectrum. First, the SHG signal in the region of the $E \rightarrow E$: O(p_x, p_y) $\rightarrow$ Ti-t_{2g}(d_{xz}, d_{yz}) transition of sp spectrum above 4 eV is nonzero. Second, the $E \rightarrow B_2$: O(p_x, p_y) $\rightarrow$ Ti-t_{2g}(d_{xy}) transition of the ds and pp spectra below 4 eV is allowed which may explain the slightly different spectral shape of these spectra in comparison to the SrO-terminated samples.

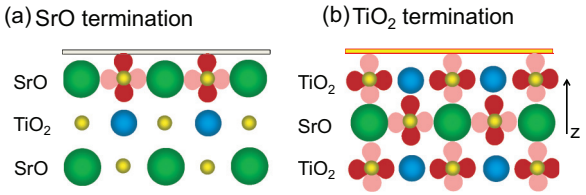

FIG. 4. (Color online) A schematic picture of the two possible STO terminations. The oxygen $2p$ orbitals are shown in dark red and pink, where the dark-red highlights the direction maximizing the overlap with the Ti atom. In the case of the SrO-terminated STO $2p_z$ orbitals point towards the Ti atoms beneath, thus favoring the orbital overlap.

The SHG sp suppression in SrO-terminated samples is a striking confirmation of our assumption that only the STO topmost atomic plane at the interface is significantly polarized in this case. This in turn implies that no significant charge injection occurs in SrO-terminated samples, as opposed to the TiO_2-terminated samples. This is also confirmed by the observation that the overall SHG intensity in SrO-terminated interfaces has roughly the same intensity as in bare STO surfaces, for which there is no charge injection, or in n-type samples with one unit cell of LAO, for which charge injection is highly unlikely. We stress that this space-charge effect is independent of the mobility and sign of the injected charges, and it would occur even if all charges were localized and/or generated from hole doping as expected for p-type interfaces. Therefore, our findings based on SHG go beyond the previously reported results of transport measurements, which revealed only the absence of mobile charges at the SrO-terminated interface.

VI. CONCLUSIONS

In summary, SHG spectra from LAO/STO interfaces showed unprecedented sensitivity on the interfacial termination. Whereas for the TiO_2-terminated surface the intensity and spectral distribution of the SHG signal indicated the presence of charge injection at the interface, in the case of SrO termination a spectrally selective and very efficient suppression of SHG yield reveals that no injection of either mobile or localized charge occurs (with the possible exception of the first atomic plane). Hence, the lack of conduction in SrO-terminated LAO/STO interfaces cannot be ascribed to a disorder-induced charge localization effect. This result was derived from a rigorous application of symmetries and selection rules to the electronic transitions between the O($2p$)

and Ti($3d$) orbitals near the STO band gap. Our findings are important for achieving a complete understanding of the physics of this complex system.

ACKNOWLEDGMENTS

We acknowledge funding from the European Union (Programme FP7/2007-2013, Grant Agreements No. 264098–MAMA and No. 228989-OxIDes), by the Ministero dell'Istruzione, dell'Università e della Ricerca (Grant No. PRIN 2010-11-OXIDE), by the Deutsche Forschungsgemeinschaft (SFB 608 and TRR 80), and by the Swiss National Science Foundation through the National Center of Competence in Research, Materials with Novel Electronic Properties, MaNEP and division II.

*domenico.paparo@spin.cnr.it

[1] A. Ohtomo and H. Hwang, Nature (London) **427**, 423 (2004).
[2] P. Zubko, S. Gariglio, M. Gabay, P. Ghosez, and J.-M. Triscone, Annu. Rev. Condens. Matter Phys. **2**, 141 (2011).
[3] N. Nakagawa, H. Y. Hwang, and D. A. Muller, Nat. Mater. **5**, 204 (2006).
[4] G. Herranz, M. Basletic, M. Bibes, C. Carretero, E. Tafra, E. Jacquet, K. Bouzehouane, C. Deranlot, A. Hamzic, J. M. Broto, A. Barthelemy, and A. Fert, Phys. Rev. Lett. **98**, 216803 (2007).
[5] W. Siemons, G. Koster, H. Yamamoto, W. A. Harrison, G. Lucovsky, T. H. Geballe, D. H. A. Blank, and M. R. Beasley, Phys. Rev. Lett. **98**, 196802 (2007).
[6] A. Kalabukhov, R. Gunnarsson, J. Borjesson, E. Olsson, T. Claeson, and D. Winkler, Phys. Rev. B **75**, 121404 (2007).
[7] K. Yoshimatsu, R. Yasuhara, H. Kumigashira, and M. Oshima, Phys. Rev. Lett. **101**, 026802 (2008).
[8] S. A. Pauli and P. R. Willmott, J. Phys.: Condens. Matter **20**, 264012 (2008).
[9] A. S. Kalabukhov, Y. A. Boikov, I. T. Serenkov, V. I. Sakharov, V. N. Popok, R. Gunnarsson, J. Borjesson, N. Ljustina, E. Olsson, D. Winkler, and T. Claeson, Phys. Rev. Lett. **103**, 146101 (2009).
[10] S. A. Chambers, M. H. Engelhard, V. Shutthanandan, Z. Zhu, T. C. Droubay, L. Qiao, P. V. Sushko, T. Feng, H. D. Lee, T. Gustafsson, E. Garfunkel, A. B. Shah, J. M. Zuo, and Q. M. Ramasse, Surf. Sci. Rep. **65**, 317 (2010).
[11] Z. Q. Liu, C. J. Li, W. M. Lü, X. H. Huang, Z. Huang, S. W. Zeng, X. P. Qiu, L. S. Huang, A. Annadi, J. S. Chen, J. M. D. Coey, T. Venkatesan, and Ariando, Phys. Rev. X **3**, 021010 (2013).
[12] S. Thiel, G. Hammerl, A. Schmehl, C. Schneider, and J. Mannhart, Science **313**, 1942 (2006).
[13] M. L. Reinle-Schmitt, C. Cancellieri, D. Li, D. Fontaine, M. Medarde, E. Pomjakushina, C. W. Schneider, S. Gariglio, P. Ghosez, J. M. Triscone, and P. R. Willmott, Nat. Commuun. **3**, 932 (2012).
[14] C. Cancellieri, D. Fontaine, S. Gariglio, N. Reyren, A. D. Caviglia, A. Fete, S. J. Leake, S. A. Pauli, P. R. Willmott, M. Stengel, P. Ghosez, and J. M. Triscone, Phys. Rev. Lett. **107**, 056102 (2011).
[15] S. A. Pauli, S. J. Leake, B. Delley, M. Bjorck, C. W. Schneider, C. M. Schleputz, D. Martoccia, S. Paetel, J. Mannhart, and P. R. Willmott, Phys. Rev. Lett. **106**, 036101 (2011).
[16] C. Cantoni, J. Gazquez, F. M. Granozio, M. P. Oxley, M. Varela, A. R. Lupini, S. J. Pennycook, C. Aruta, U. Scotti di Uccio, P. Perna, and D. Maccariello, Adv. Mater. **24**, 3952 (2012).
[17] C. Cancellieri, N. Reyren, S. Gariglio, A. D. Caviglia, A. Fete, and J.-M. Triscone, Europhys. Lett. **91**, 17004 (2010).
[18] A. Savoia, D. Paparo, P. Perna, Z. Ristic, M. Salluzzo, F. Miletto Granozio, U. Scotti di Uccio, C. Richter, S. Thiel, J. Mannhart, and L. Marrucci, Phys. Rev. B **80**, 075110 (2009).
[19] N. Ogawa, K. Miyano, M. Hosoda, T. Higuchi, C. Bell, Y. Hikita, and H. Y. Hwang, Phys. Rev. B **80**, 081106(R) (2009).
[20] A. Rubano, M. Fiebig, D. Paparo, A. Marino, D. Maccariello, U. Scotti di Uccio, F. Miletto Granozio, L. Marrucci, C. Richter, S. Paetel, and J. Mannhart, Phys. Rev. B **83**, 155405 (2011).
[21] T. Günter, A. Rubano, D. Paparo, M. Lilienblum, L. Marrucci, F. Miletto Granozio, U. Scotti di Uccio, R. Jany, C. Richter, J. Mannhart, and M. Fiebig, Phys. Rev. B **86**, 235418 (2012).
[22] W. Luo, W. Duan, S. G. Louie, and M. L. Cohen, Phys. Rev. B **70**, 214109 (2004).
[23] A. H. Kahn and A. J. Leyendecker, Phys. Rev. **135**, A1321 (1964).
[24] M. Salluzzo, J. C. Cezar, N. B. Brookes, V. Bisogni, G. M. De Luca, C. Richter, S. Thiel, J. Mannhart, M. Huijben, A. Brinkman, G. Rijnders, and G. Ghiringhelli, Phys. Rev. Lett. **102**, 166804 (2009).
[25] D. C. Harris and M. D. Bertolucci, *Symmetry and Spectroscopy: An Introduction to Vibrational and Electronic Spectroscopy* (Dover, New York 1989).
[26] K. van Benthem, C. Elsässer, and R. H. French, J. Appl. Phys. **90**, 6156 (2001).
[27] A. F. Santander-Syro, O. Copie, T. Kondo, F. Fortuna, S. Pailhes, R. Weht, X. G. Qiu, F. Bertran, A. Nicolaou, A. Taleb-Ibrahimi, P. Le Fevre, G. Herranz, M. Bibes, N. Reyren, Y. Apertet, P. Lecoeur, A. Barthelemy, and M. J. Rozenberg, Nature (London) **469**, 189 (2011).
[28] M. Basletic, J. L. Maurice, C. Carretero, G. Herranz, O. Copie, M. Bibes, E. Jacquet, K. Bouzehouane, S. Fusil, and A. Barthelemy, Nat. Mater. **7**, 621 (2008).